2024 IEEE International Conference on Robotics and Automation (ICRA 2024)
May 13-17, 2024. Yokohama, Japan

Nature-Inspired Bubble Magnetic Microrobots for Multimode Locomotion, Cargo delivery, Imaging, and Biosensing

Zichen Xu, Qingsong Xu, *Senior Member, IEEE*, and Hon Ho Yu

***Abstract*— Wirelessly actuated magnetic microrobots are promising tools in medical applications due to their tiny sizes and attractive robotic properties. However, it remains a huge challenge to integrate sufficient functionalities in a limited volume. Microscopic natural phenomenon is a great reference for current microrobot design, where the underlying intelligence and subtlety spurs related modern artificial systems. Inspired by air bubbles in nature, herein, we report a kind of novel magnetic air bubble microrobots. The air bubble-based structure enables multiple functionalities including cargo delivery, multimode locomotion, micromanipulation, medical imaging, and biosensing. The proposed microrobot is essentially Pickering bubbles composed of magnetic particles and air bubbles. Their hollow structures help produce lighter microrobots with density less than 1 g/cm^3, enabling buoyancy-based self-propulsion. Buoyancy and magnetic forces actuation enables flexible 3D locomotion in fluidic environments. Experimental results show that the microrobots can be controlled properly for designated assignments. Furthermore, the introduction of air bubble enhances ultrasound imaging, facilitating further in vivo applications. These findings offer a significant microrobot design paradigm by exploiting natural physical intelligence at the small scale.**

I. INTRODUCTION

Wireless-actuated magnetic microrobots have demonstrated attractive performances in plenty of medical applications, ranging from target drug delivery to invasive surgeries, which enables robotic operations at crowded corners within deep human tissues [1], [2]. However, the limited size and volume hinder more functional integrations in current microrobot study [3]. It is desirable to achieve more functionalities as much as possible in a constrained space [4]. Oberserving microscopic natural phenomena, the underlying intelligence and subtlety provides valuable inpsirations to utilize simple structures to achieve complex functionalities, such as air bubbles. Bubbles can scavenge biogenic organics in marine [5], enable underwater sniffing for animals [6], and even possibly contribute to the origin of life on Earth [7], demonstrating intriguing performance in matter delivery, information access, and so on, ranging from micro to macro scale. Similar to the normal-sized robots, medical microrobots require necessary abilities in locomotion, perception, navigation, execution, and sensing [8]–[12], which is significant to achieve their clinical functionalities [15], [17]. However, their limited sizes severely hinder functional implementation and integration, such as the lack of volume for on-board components [13], [14], [18], [19]. In fact, the minimization of those functional components has always been a hot research topic, ranging from sensors [20] to actuators [21]. At the small scale, it is difficult to manufacture and assemble microrobots using traditional macro-processing method [10], [22], [23]. The intelligence of microrobots mainly relies on functional materials [24], relatively simple mechanical designs, or biological factors [16], which is insufficient for complex medical assignments. Essentially, majority of microrobotic phenomena can be regarded as pure physical procedures [25], [26]. To exploit the microscopic physical interactions, bubble is a promising strategy for enabling microrobot designs by introducing underlying physical intelligence to widen microrobots' functionalities.

Herein, we propose a microrobot constructed by micro air bubble (100 μm or less) with μm-level magnetic hydrophobic microparticles (iron-nickel alloy) adsorbed on the bubble surface. It is a pure physical procedure and also known as Pickering bubble [27]–[29]. Such a novel microrobot design demonstrates attractive performances and properties in cargo delivery, multimode locomotion, micromanipulation, medical imaging, and biosensing. For cargo delivery, hydrophobic objects are well captured by water-air interface interactions, guaranteeing the cargo integrity during navigating in a flowing medium. By applying a 100-mT level magnetic field, microparticles are separated from the air bubble, realizing cargo release. It is a reliable method in fast flowing environments to deliver numerous microparticles and release them. For locomotion, the air bubble-based structure contributes to generating microrobots with different density, enabling flexible switch of buoyancy-based self-propulsion and magnetic actuation for 3D navigation. In fluidic environments, the self-propulsion speed can reach 70 body length per second (or more). For the tasks cannot be fulfilled by single individuals, multiple air bubble microrobots are organized in various formations. In addition, the air bubble structure promotes the efficiency of ultrasound observation, facilitating in vivo applications.

By selecting proper hydrophobic particles and gas bubbles, with the help of several gas-liquid reactions, the microrobots' shape or structures can well reflect the fluidic environmental properties, such as the pH value. Thus, this novel design

This work was supported in part by National Natural Science Foundation of China under Grant 52175556, the Macao Science and Technology Development Fund under Grant 0004/2022/AKP and 0102/2022/A2, the University of Macau under Grant MYRG2022-00068-FST and MYRG-CRG2022-00004-FST-ICI, and the Guangdong Basic and Applied Basic Research Foundation under Grant 2023A1515011178.

Z. Xu and Q. Xu are with the Department of Electromechanical Engineering, Faculty of Science and Technology, University of Macau, Avenida da Universidade, Taipa, Macau, China.

H. H. Yu is with the Department of Gastroenterology, Kiang Wu Hospital, Est. Coelho Amaral 62, Macau, China.

Corresponding author: Qingsong Xu (e-mail: qsxu@um.edu.mo; phone: +853-88224278; fax: +853-88222426).

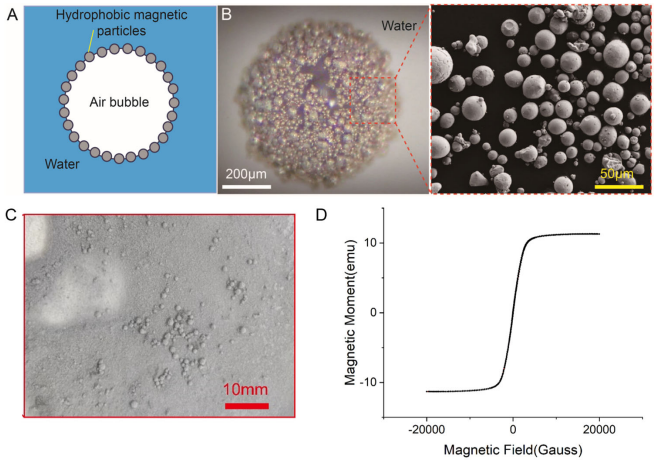

Fig. 1. Schematic and experimental images of magnetic air bubble microrobots. (A) Schematic of a magnetic air bubble microrobot. (B) Experimental image of a magnetic air bubble microrobot. Numerous particles are adsorbed on the air bubble surface to formulate the microrobot. (C) Images of the generated magnetic air bubble microrobots. (D) Magnetic hysteresis loop indicating the microparticles' magnetization properties.

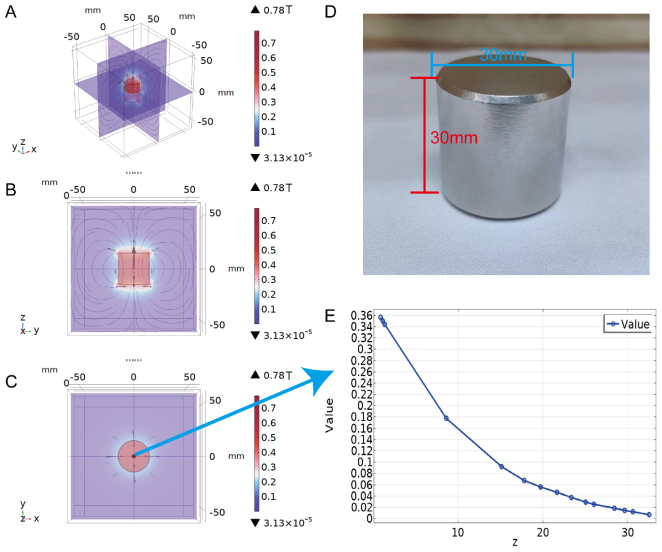

Fig. 2. Detailed information of the utilized NdFeB permanent magnet. (A)-(C) COMSOL simulation results of the magnet. (D) Actual image of the utilized magnet. (E) Simulated value results indicate the magnetic field density distribution in the z-axis direction at the point in (C). The unit of the value is T, and z denotes the distance from the magnet surface (unit: mm).

is promising to enable more functionalities in clinics in future, including sensing, treatment, detection, and imaging. Our findings offer a new microrobot design paradigm by exploiting the physical intelligence at the small scale.

II. Microrobot Fabrication and Experimental Setup

A. Microrobot Fabrication

Essentially, the magnetic air bubble microrobots are a kind of Pickering bubbles, whose generation is due to the collective effects of collision, attachment, and balance of relative interactions between magnetic hydrophobic microparticles and air bubble. For the bubbles to capture hydrophobic particles, the distance between them should be close enough, so that related attractive surface interactions can make effects [30], [31]. The whole process is somewhat random and it is difficult to precisely control the size of the generated microrobots.

In the experiments, the magnetic microparticles were composed of 300-mesh iron-nickel alloy (Fig. 1A&B). The outstanding magnetization of these microparticles was critical for achieving robotic tasks (Fig. 1D). Without other processing, we added 1–2 g microparticles in a small vial (3 mL or 5 mL). Then, we added approximately 2 mL of pure water to the vial and shook it by hand for 30 s. After placing the suspension for 1-2 minutes, we observed several magnetic air bubble microrobots (Fig. 1C). In addition, the air bubble-based structures are hollow, contributing to great variation in density. To simplify the circulation, the density (ρ_m) of microrobots can be described as:

$$\rho_m = \frac{6\bar{r_p}\rho_p C}{R} \tag{1}$$

where $\bar{r_p}$, ρ_p, R, and C represent the mean radius of the particles adsorbed on the airibubble surface, density of the particles, radius of the microrobot (or air bubble), and cover coefficient indicating the encapsulation of particles to bubbles, respectively.

B. Magnetic Actuation

The introduction of magnetic particles is a key factor to empower Pickering bubbles with robotic properties. Magnetic microrobots can be actuated by external magnetic fields through magnetic forces and torques. As shown in Fig. 2, magnetic forces can be easily generated by permanant magnets as follows [32].

$$F_m = \int_{V_m} (M \cdot \nabla) B dV_m \tag{2}$$

where V_m, M, and B denote the volume of the magnetized object (which is essentially the particles adsorbed on the air bubble surface), magnetization of the object, and flux density of the magnetic field, respectively.

As shown in Fig. 3, magentic torques are supplied by well-designed electromagnetic coils as follows.

$$\tau_m = \int_{V_m} M \times B dV_m \tag{3}$$

Microrobots with different densities are supposed to be actuated by different means. Related simulation results are provided in Fig. 4. It is observed that relatively large microrobots (diameter $>$ 0.8 mm) float near the water-air surface, and relatively small microrobots (diameter $<$ 0.7 mm) sink to the bottom. Microrobots with different sizes have various dynamic properties, whereas microrobots near the water-air interface easily actuate. Weak magnetic fields (10 mT level) are able to actuate those microrobots. Due to the lack of contact with the terrain surface for relatively light microrobots that float upwards, we prefer to apply proper

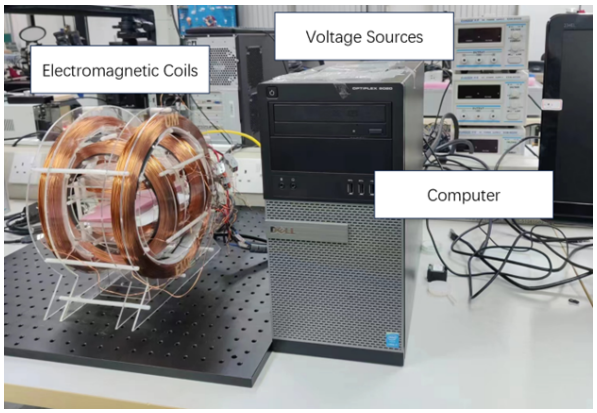

Fig. 3. Prototype and experimental setup for the electromagnetic coils to achieve precise motion control of the microrobots.

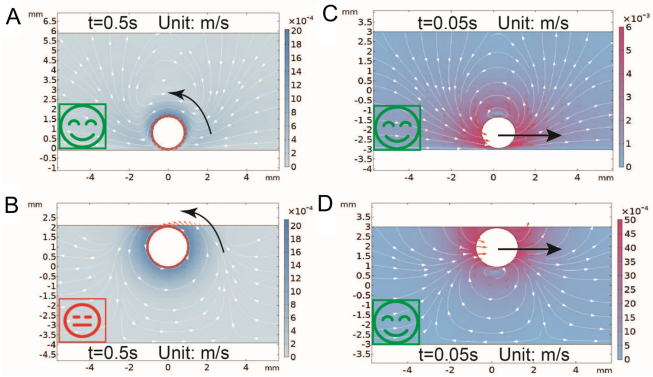

Fig. 4. COMSOL simulation results. (A) The controlled rotation movement near the glass surface underwater. (B) The controlled rotation movement near the water-air interface. (C) The controlled parallel movement near the glass surface underwater. (D) The controlled parallel movement near the water-air interface.

magnetic forces instead of magnetic torques for actuation. For magnetic torque actuation, microrobots are rotated to generate propulsion. The magnetic air bubble microrobots can be regarded as microrollers in the rotation motion. In the fluidic environment, microrobots' rotation motion contributes to the hydrodynamics mismatch near the wall, causing translational motion, where related velocity response is presented in Fig. 5. Without necessary contact with walls, the rotation of microrobots cannot generate translational motion.

III. Experimental Results

A. Multimode Locomotion Results

In medical applications, fluidic environments are the main scenarios, such as vascular systems. In flowing medium, the microrobots need to go downstream or upstream to reach desired places. It is crucial to enable microrobots' smooth downstream locomotion in the circulatory system, which can carry microrobots to lots of tissues, simplifying part of microrobotic navigation tasks. The density of microrobot is relatively low due to the air bubble-based structure, reducing gravity induced near-wall interactions . In the glass tube with inner diameter of 1.3 mm, the microrobot (diameter: 800 μm)

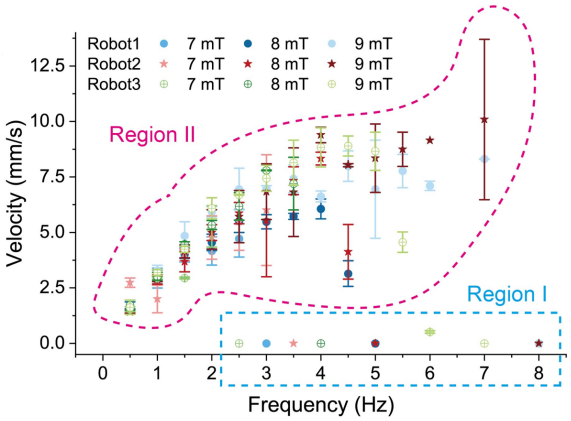

Fig. 5. Velocity responses to different external rotation magnetic fields for three microrobots with different sizes. In region I, microrobots cannot be well actuated due to the great increase of the frequency. In region II, microrobots can be well actuated.

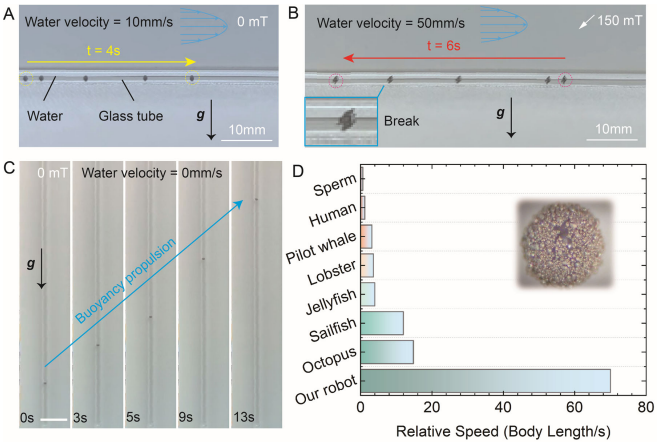

Fig. 6. Microrobots' multimode locomotion in fluidic environments. (A) Microrobot goes downstream following the flowing medium (10 mm/s) without magnetic actuation. (B) Magnetic actuation enables the microrobot to go upstream against the flowing medium (50 mm/s) in the glass tube (inner diameter: 1.3 mm). (C) Microrobot's buoyancy-based self-propulsion (Scalar bar: 5 mm). (D) Relative speed comparison among microrobots and various creatures.

went downstream smoothly in slow flowing water (10 mm/s), without adhesion to the inner surface (Fig. 6A). In fact, a magnetic field of 30 mT level is able to stop the microrobot at designated position in the flowing water (50 mm/s), and a magnetic field of 150 mT level can even drive the microrobot to navigate upstream with broken structure, where strong magnetic fields make the microrobot break (Fig. 6B).

Furthermore, except for magnetic actuation, the microrobots with smaller density ($<$1 g/cm^3) demonstrate attractive performance in self-propulsion in fluidic environment, where the buoyancy is the key factor. By modifying the position of terrain, such as channel directions, the buoyancy can drive the microrobots against gravity direction, achieving self-propulsion navigation (Fig. 6C). In the channel whose radius is much larger (over 10 times) than the microrobot's size, the self-propulsion speed can even reach 70 body length per second (Fig. 6D). For example, by modifying

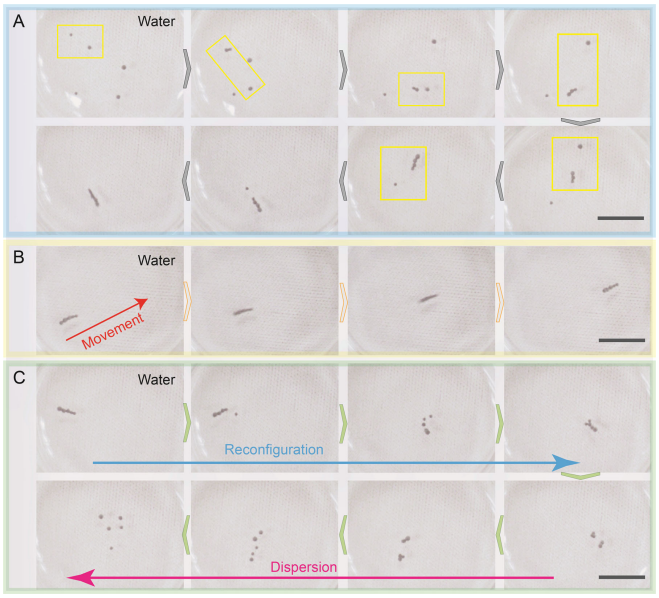

Fig. 7. Generation and actuation of magnetic air bubble microrobots. (A) Chain-like microrobot swarm generation. (B) The controlled movement of chain-like microrobot swarm. (C) Microrobot swarm reconfiguration and dispersion.

the direction of vessels and gravity direction, it is able to control the microrobots' moving direction and speed relative to the vessels. For clinical scenarios, it is accessible to change the patients position relative to gravity direction. It is a brand new microrobot actuation strategy which brings an alternative solution to achieve microrobot locomotion in fluidic environments.

B. Results of Swarming Strategy

Microrobot swarming strategy is an effective method to promote the microrobots' performance to cope with tough assignments that are almost impossible to single microrobot individuals due to the limited volume and size. Considering that the magnetic actuation is provided by a permanent NdFeB magnet (diameter: 30 mm, height: 30 mm), we put forward a special swarming strategy under this circumstance. Inhomogeneous magnetic fields are utilized to organize the microrobots with different sizes. The swarming procedure can be described that microrobots are converged by applying magnetic forces with designated directions. The convergence directions follow the magnetic field gradient direction, namely, the magnetic force direction. We adopt a step-by-step method to organize microrobots in chain-like structure one by one (Fig. 7A). Single microrobots have no specific orientation. When two microrobots are combined, they form a small chain along the magnetic field direction. After tuning the direction of the small chain and make it point to the next microrobot individual, we move the magnet to approach those three microrobots, where they follow the same direction and converge to form a bigger chain composed of three microrobots. Following this process, it is able to organize them to generate chain-like structures. The chain-like swarm helps microrobots to work together toward complex assignments (Fig. 7B). Microrobots converging in one direction forms the chain-like structures, and microrobot converging in multiple directions can form more interesting structures, namely, a chain-like structure with several branches (Fig. 7C). To disorder those organized swarms, we can utilize a magnet to provide inhomogeneous oscillation magnetic fields, which brings the outer microrobots far away from the main part of microrobot swarm (Fig. 7C). This strategy further promotes the performance of the designed microrobots.

C. Cargo Delivery Results

The interface interactions near the air bubble are significant and strong to capture objects. Thus, the air bubble microrobots own the ability to load cargos and deliver them. In addition, the air bubble microrobot with smaller density helps to carry micro-objects to navigate smoothly in 3D space, especially in the gravity direction (Fig. 8B&C). Considering more specific application scenarios, such as digestive systems, the mucus and cilia on tissue surface severely hinder the microrobot's navigation and its cargo delivery. To solve this problem, we utilize lighter microrobot that can float near the water-air interface, where its navigation avoids the contact with tissue surface and promote the delivery efficiency. After arriving at the top of the desired position, we utilize strong magnetic fields (150 mT) to release bubble and particles on the target surface (Fig. 8C).

D. Imaging and Biosensing Results

It is significant to guarantee the control and observation stability of microrobot functionalities in environments (Fig. 9A). Experiments were conducted in artificial blood to achieve microrobots' swiftly controlled movement (Fig. 9B). From a medical imaging application perspective, microbubbles perform well to enhance imaging results. Using an ultrasound equipment, a microrobot (diameter of approximately 1 mm) can be clearly observed in a plastic tube full of water (Fig. 9C), which is vital for in vivo medical applications. This microrobot can stay stable in artificial blood for 3 days, proving its stability. The volume of a gas is easier to change than that of a liquid or solid, making the gas more intuitive and possible to implement. On this basis, bubbles can serve as microsensors to reflect the properties of fluidic environments. Herein, we utilize the liquid-gas reaction between CO_2 gas and NaOH solution to design microrobot-based biosensors. The microrobot is produced by a CO_2 bubble instead of an air bubble. Its size is reduced once contacting with alkaline environments (Fig. 9D). By observing the shapes of microrobots, we can obtain the pH value of fluidic environments.

By considering the in vivo observation of bubbles, we find that this biosensing method is promising for future detection of medical applications. The applicability to biosensing can be enhanced by selecting different gases. According to the above experiments, we have succeeded in designing novel

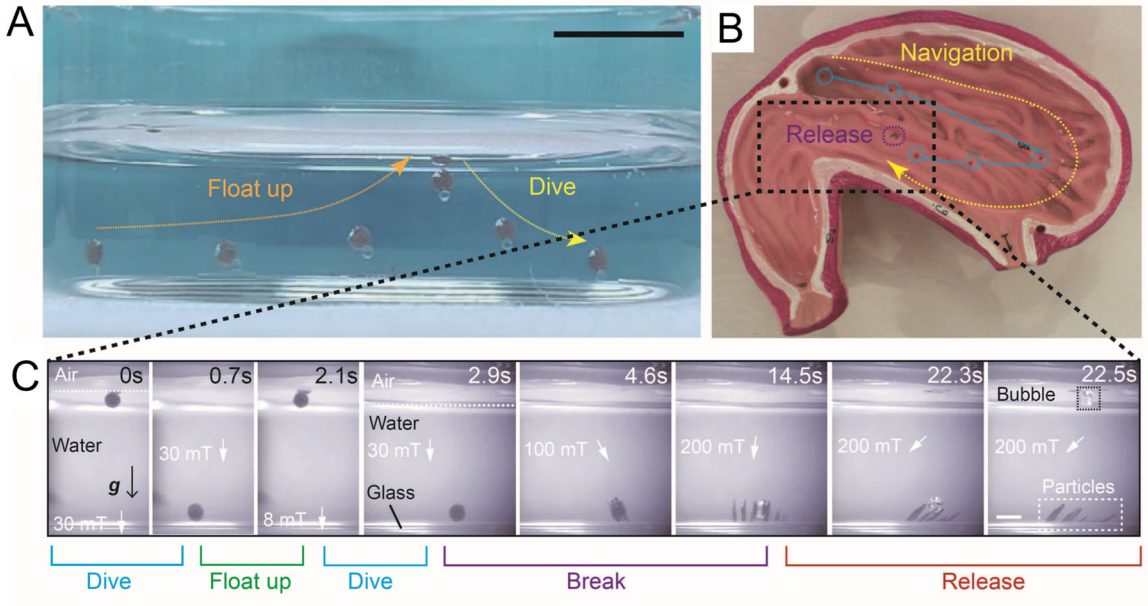

Fig. 8. Controlled cargo delivery and on-demand release in extreme environments. (A) Microrobot carrying micro-objects to achieve flexible 3D navigation. (B) Microrobot navigating smoothly in a stomach model and releasing particles in designated places under complex terrain conditions. (C) Controlled movement of the microrobot in the direction of gravity and the release of surface magnetic hydrophobic microparticles (scale bar: 2 mm).

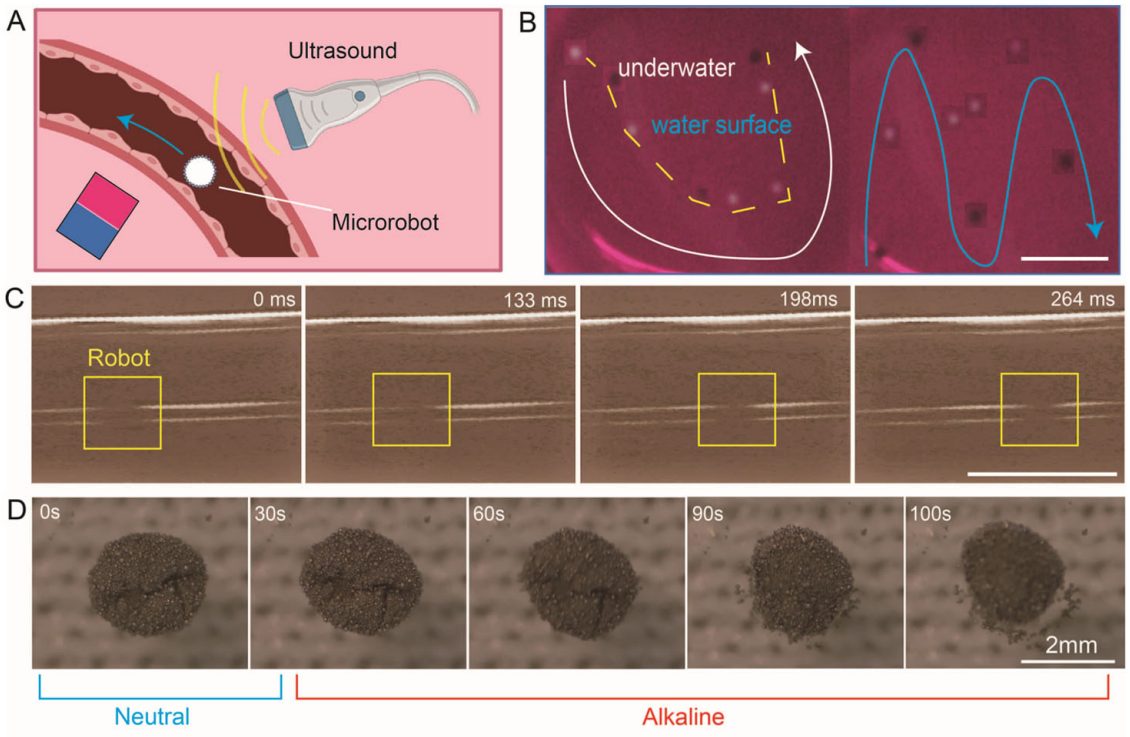

Fig. 9. Medcal imaging and biosening in the vessel. (A) Schematic of microrobot navigation in the vessel under the guidance of ultrasound equipment. (B) Controlled 3D navigation of the microrobot in artificial blood. The microrobot's diameter is approximately 0.8 mm (scale bar: 5 mm). (C) Ultrasound-guided locomotion results. In the yellow boxes, the microrobot position can be easily observed. (D) Biosensing test results. The microrobot composed of CO_2 gas experiences shape changes in alkaline environments (unless otherwise specified, all scale bars are 10 mm).

microrobots that can achieve cargo loading, cargo delivery, medical imaging, and biosensing simultaneously.

IV. Conclusion

In this paper, we present a novel design of magnetic air bubble microrobots that achieves multiple functionality integration, and enhances the ability in locomotion, delivery, medical imaging, and biosensing. It provides a great reference to exploit the physical intelligence underlying in natural phenomenon. By incorporating air bubbles that adsorb particles, we have successfully mitigated particle loss in fluidic environments to some extent. Moreover, while magnetic particle collectives encounter challenges in achieving 3D space navigation and moving across biological tissue surfaces, air bubbles act as "submarines", facilitating more flexible locomotion by circumventing barriers. This integration of gas bubbles significantly enriches the microrobots' functionalities. The introduction of air bubbles plays a pivotal role in enhancing microrobot stability during cargo delivery by promoting strong interactions at the air-water interface, ensuring tight and secure particle adhesion to objects. Furthermore, air bubbles organize microparticles into a spherical shell, enhancing microrobot visualization and ultrasound imaging efficiency for more precise in vivo treatment. In the future, we will further exploit the physical interactions for microrobots from theory to application to develop detailed and precise clinical applications and enhance existing microrobot performance attributes.

References

[1] Y. Kim and X. Zhao, "Magnetic Soft Materials and Robots," *Chemical Reviews*, vol. 122, no. 5, pp. 5317-5364, 2022.

[2] H. Lu, M. Zhang, Y. Yang, Q. Huang, T. Fukuda, Z. Wang, and Y. Shen, "A bioinspired multilegged soft millirobot that functions in both dry and wet conditions," *Nat. Commun.*, vol. 9, no. 1, pp. 3944, 2018.

[3] Z. Xu and Q. Xu, "Collective behaviors of magnetic microparticle swarms: From dexterous tentacles to reconfigurable carpets," *ACS Nano*, vol. 16, no. 9, pp. 13728-13739, 2022.

[4] Z. Xu, Y. Chen, and Q. Xu, "Spreadable magnetic soft robots with on-demand hardening," *Research*, vol. 6, Art. no. 0262, 2023.

[5] T. W. Wilson, L. A. Ladino, P. A. Alpert, et al., "A marine biogenic source of atmospheric ice-nucleating particles," *Nature*, vol. 525, no. 7568, pp. 234-238, 2015.

[6] K. C. Catania, "Underwater 'sniffing' by semi-aquatic mammals," *Nature*. vol. 444, pp. 1024-1025, 2006.

[7] T. Z. Jia, K. Chandru, Y. Hongo, and H. J. Cleaves II, "Membraneless polyester microdroplets as primordial compartments at the origins of life," *Proc. Natl. Acad. Sci. U. S. A.*, vol. 116, no. 32, pp. 15830-15835, 2019.

[8] Q. Wang, K. F. Chan, K. Schweizer, X. Du, D. Jin, S. C. H. Yu, B. J. Nelson, and L. Zhang, "Ultrasound Doppler-guided real-time navigation of a magnetic microswarm for active endovascular delivery," *Sci. Adv.*, vol. 7, no. 9, Art. no. eabe5914, 2021.

[9] X. Yang, W. Shang, H. Lu, Y. Liu, L. Yang, R. Tan, X. Wu, and Y. Shen, "An agglutinate magnetic spray transforms inanimate objects into millirobots for biomedical applications," *Sci. Robot.*, vol. 5, no. 48, Art. no. eabc8191, 2020.

[10] J. Zhang, Z. Ren, W. Hu, R. H. Soon, I. C. Yasa, Z. Liu, and M. Sitti, "Voxelated three-dimensional miniature magnetic soft machines via multimaterial heterogeneous assembly," *Sci. Robot.*, vol. 6, no. 53, Art. no. eabf0112, 2021.

[11] J. Li, B. E.-F. de Avila, W. Gao, L. Zhang, and J. Wang, "Micro/nanorobots for biomedicine: Delivery, surgery, sensing, and detoxification," *Sci. Robot.*, vol. 2, Art. no. eaam6431, 2017.

[12] Z. Wu, L. Li, Y. Yang, P. Hu, Y. Li, S.-Y. Yang, L. V. Wang, and W. Gao, "A microrobotic system guided by photoacoustic computed tomography for targeted navigation in intestines in vivo," *Sci. Robot.*, vol. 4, Art. no. eaax0613, 2019.

[13] W. Hu, G. Z. Lum, M. Mastrangeli, and M. Sitti, "Small-scale soft-bodied robot with multimodal locomotion," *Nature*, vol. 554, no. 7690, pp. 81-85, 2018.

[14] P. Wrede, O. Degtyaruk, S. K. Kalva, X. L. Dean-Ben, U. Bozuyuk, A. Aghakhani, B. Akolpoglu, M. Sitti, and D. Razansky, "Real-time 3D optoacoustic tracking of cell-sized magnetic microrobots circulating in the mouse brain vasculature," *Sci. Robot.*, vol. 8, Art. no. eabm9132, 2022.

[15] S. Jeon, S. Kim, S. Ha, S. Lee, E. Kim, S. Y. Kim, S. H. Park, J. H. Jeon, S. W. Kim, C. Moon, B. J. Nelson, J.-y. Kim, S.-W. Yu, and H. Choi, "Magnetically actuated microrobots as a platform for stem cell transplantation," *Sci. Robot.*, vol. 4, Art. no. eaav4317, 2019.

[16] X. Yan, Q. Zhou, M. Vincent, Y. Deng, J. Yu, J. Xu, T. Xu, T. Tang, L. Bian, Y.-X. J. Wang, K. Kostarelos, and L. Zhang, "Multifunctional biohybrid magnetite microrobots for imaging-guided therapy," *Sci. Robot.*, vol. 2, Art. no. eaaq1155, 2017.

[17] B. Wang, K. F. Chan, K. Yuan, Q. Wang, X. Xia, L. Yang, H. Ko, Y.-X. J. Wang, J. J. Y. Sung, P. W. Y. Chiu, and L. Zhang, "Endoscopy-assisted magnetic navigation of biohybrid soft microrobots with rapid endoluminal delivery and imaging," *Sci. Robot.*, vol. 6, Art. no. eabd2813, 2021.

[18] J. Yu, B. Wang, X. Du, Q. Wang, and L. Zhang, "Ultra-extensible ribbon-like magnetic microswarm," *Nat. Commun.*, vol. 9, Art. no.5749, 2018.

[19] D. Ahmed, A. Sukhov, D. Hauri, D. Rodrigue, G. Maranta, J. Harting, and B. J. Nelson, "Bioinspired acousto-magnetic microswarm robots with upstream motility," *Nat. Mach. Intell.*, vol. 3, no. 2, pp. 116-124, 2021.

[20] B. Gleich, I. Schmale, T. Nielsen, and J. Rahmer, "Miniature magneto-mechanical resonators for wireless tracking and sensing," *Science*, vol. 380, no. 6648, Art no. 966-971, 2021.

[21] T. Nitta, Y. Wang, Z. Du, K. Morishima, and Y. Hiratsuka, "A printable active network actuator built from an engineered biomolecular motor," *Nat. Mater.*, vol. 20, no. 8, pp. 1149-1155, 2021.

[22] N. Xia, D. Jin, C. Pan, J. Zhang, Z. Yang, L. Su, Ji. Zhao, L. Wang, and L. Zhang, "Dynamic morphological transformations in soft architected materials via buckling instability encoded heterogeneous magnetization," *Nat. Commun.*, vol. 13, Art. no. 7514, Dec. 2022.

[23] T. Xu, J. Zhang, M. Salehizadeh, O. Onaizah, and E. Diller, "Millimeter-scale flexible robots with programmable three-dimensional magnetization and motions," *Sci. Robot.*, vol. 4, no. 29, 2019, doi: 10.1126/scirobotics.aav4494.

[24] M. Sun, B. Hao, S. Yang, X. Wang, C. Majidi, and L. Zhang, "Exploiting ferrofluidic wetting for miniature soft machines," *Nat. Commun.*, vol. 13, no. 1, Dec. 2022.

[25] Z.H. Wu, Y. Zhang, N. Ai, H. Chen, W. Ge, and Q. Xu, "Magnetic Mobile Microrobots for Upstream and Downstream Navigation in Biofluids with Variable Flow Rate," *Advanced Intelligent Systems*, vol. 4, no. 7, Art. no. 2100266, 2022.

[26] Y. Wei, Z. Wu, Z. Dai, B. Zhou, and Q. Xu, "Design of a Magnetic Soft Inchworm Millirobot Based on Pre-strained Elastomer with Microcilias," *Biomimetics*, vol. 8, no. 1, Art. no. 22, 2023.

[27] P. Amani, R. Miller, A. Javadi, and M. Firouzi, "Pickering foams and parameters influencing their characteristics," *Advances in Colloid and Interface Science*, vol. 301, pp. 102606, 2022.

[28] E. Blanco, S. Lam, S. K. Smoukov, K. P. Velikov, S. A. Khan, and O. D. Velev, "Stability and viscoelasticity of magneto-pickering foams," *Langmuir*, vol. 29, no. 32, pp. 10019-10027, 2013.

[29] Y. Gao, C. U. Chan, et al., "Controlled nanoparticle release from stable magnetic microbubble oscillations," *NPG Asia Materials*, vol. 8, no. 4, Art. no. e260, 2016.

[30] J. Ralston and S. S. Dukhin, "The interaction between particles and bubbles," *Colloids Surf. A Physicochem Eng. Asp.*, vol. 151, pp. 3-14, 1999.

[31] D. Wu, V. Mihali, and A. Honciuc, "pH-Responsive Pickering Foams Generated by Surfactant-Free Soft Hydrogel Particles," *Langmuir*, vol. 35, pp. 212–221 2019.

[32] Z. Xu, Z. Wu, M. Yuan, Y. Chen, W. Ge, and Q. Xu, "Versatile magnetic hydrogel soft capsule microrobots for targeted delivery," *iScience*, vol. 26, no. 5, Art. no. 106727, 2023.